Sensors and Materials, Vol. 34, No. 4 (2022) 1433–1444
MYU Tokyo

S & M 2901

Novel Sub-area Maximum Power Point Tracking Method Based on Improved Variable-step-size Perturbation and Observation

Xiaoping Lei*

College of Electronics and Internet of Things, Chongqing College of Electronic Engineering,
Chongqing 401331, China

(Received September 14, 2021; accepted January 17, 2022)

Keywords: variable step size, perturbation and observation (P&O), subarea function, maximum power point tracking (MPPT), energy harvester

The output power of photovoltaic panels fluctuates significantly with the temperature and radiation intensity. To achieve safe and stable energy harvesters, it is critical to keep the output voltage of photovoltaic panels at the maximum power point (MPP). To eliminate the limitation of both a fixed step size and the low response speed caused by the small average step size in ordinary perturbation and observation (P&O), a new sub-area-based improved variable-step-size perturbation and observation (SVS-P&O) algorithm is proposed. The working area of a power generation system is divided into two different parts using the partition function. When the operating point of the photovoltaic system is far from the MPP, a larger and fixed step size is adopted to improve the tracking speed. However, when the operating point of the photovoltaic system is close to the MPP, a variable and smaller step size is adopted to reduce the fluctuation of steady-state power. Different perturbation step sizes are used in different areas, and the step size is adjusted in real-time to track the MPP through the combination of fixed and variable step sizes. The simulation results show that the proposed SVS-P&O algorithm for MPP tracking has less oscillation at the MPP than the conventional P&O method and double the tracking speed.

1. Introduction

With the emergence of global climate change and thermal pollution, photovoltaic power generation is being increasingly widely used worldwide.(1) The energy output characteristics of photovoltaic cells are greatly affected by local changes, such as in the temperature and illumination intensity, resulting in unstable energy output and low energy efficiency. To effectively utilize solar energy, maximum power point tracking (MPPT) technology is often applied in photovoltaic power generation to optimize the output energy efficiency.(2) Photovoltaic power generation equipment includes photovoltaic cells, microactuators, controllers, sensors, and power converters, and the maximum power point (MPP) can be obtained by improving the controller algorithm and converter structure.(3) For solar photovoltaic cells, the relationships

*Corresponding author: e-mail: xiaopingleilei2@163.com
https://doi.org/10.18494/SAM3655

ISSN 0914-4935

between the output power and current and between the voltage and current can be represented by *P–U* and *V–U*, respectively. However, photovoltaic cells have a fixed MPP in a specific external environment. To improve the overall efficiency of photovoltaic power generation systems, it is necessary to add a circuit between the photovoltaic panel and the circuit load to track the MPP of photovoltaic cells.

The MPPT control of photovoltaic panels has been studied and improved by global experts and scholars. The MPPT algorithms can be roughly divided into traditional and intelligent control methods. The former include typical self-optimizing algorithms, such as incremental conductance (INC),(4) and perturbation and observation (P&O)(5) and non-self-optimizing algorithms, such as constant-voltage tracking (CVT).(6) Among them, INC realizes MPPT by controlling the instantaneous conductance increment signal; thus, high accuracy is required for the detection circuit. However, CVT has the advantage of easy implementation, but it cannot track MPP in real time to achieve a dynamic response. Compared with the INC and CVT algorithms, although P&O generates oscillation at the MPP, it has the advantages of easy implementation and a dynamic response, resulting in its widespread use in practical engineering. On the other hand, intelligent control methods, including fuzzy control, neural networks, and particle swarm optimization, have good performance, but the process is complicated, making their application limited.(7)

Many improved algorithms have been proposed to enhance the tracking speed of fixed-step P&O but the problem of power fluctuation remains.(8) For variable-step-size perturbation and observation (VS-P&O), which can misjudge and produce violent oscillation when the luminous intensity changes abruptly, Liu *et al.* combined a fixed-voltage start-up with P&O for MPPT with high starting speed and control accuracy.(9) Without simultaneously considering the swing near the MPP and the power loss, steady-state accuracy, and tracking speed, Wang *et al.* adopted an improved P&O to track MPP more rapidly and accurately.(10) Rezkallah *et al.* discussed a new type of P&O to achieve both high tracking speed and steady-state accuracy. By controlling the peak current and sampling with instantaneous values instead of average values, the system responded quickly and reduced MPP oscillation.(11)

In this paper, a sub-area-based improved variable-step-size perturbation and observation (SVS-P&O) algorithm based on the traditional P&O algorithm is proposed to achieve a safe and stable energy harvester. The algorithm combines fixed and variable step sizes to adjust the tracking step size in real-time. The SVS-P&O algorithm can quickly track the MPP upon start-up and in the environment, improving the efficiency of power generation systems.

2. Photovoltaic Cell Characteristics

2.1 Basic principle of photovoltaic cell

The principle of photovoltaic cell power generation is the photovoltaic effect, in which a photovoltaic cell converts luminous energy into electric energy by applying the photovoltaic effect of a P–N junction.(12) When sunlight strikes a solar cell, the luminous energy is absorbed by the cell, creating photoelectron–hole pairs. Under the action of the electric field in the battery, the holes and photogenerated electrons are separated, and the different charges accumulate at opposite ends of the battery, i.e., photogenerated voltage is generated, which is known as the photogenerated voltaic effect. When electrodes are installed on either side of the built-in electric field and a load is connected, a photogenerated current flows through the circuit load, thus obtaining power output. In this way, the sun's luminous energy is changed into usable electrical energy.

2.2 Equivalent circuit of photovoltaic cell

To better study and analyze the *P–U* and *I–U* characteristics of a photovoltaic system, it is necessary to establish the corresponding photovoltaic equivalent circuit. The physical meaning of the equivalent circuit is explained as follows. A solar cell generates photocurrent I_{ph} after illumination, part of which is used to cancel the junction current I_D, and the other part is used to supply the load current I. In a practical solar cell, additional resistance is inevitably introduced in both the base region and the top layer because of the electrode and contact on the front and back, as well as through the resistivity of the material itself. The current flowing through loads causes losses. In the equivalent circuit, the integrated effect can be expressed by a series resistor R_s. Owing to the leakage of the battery edge, part of the current that should pass through the load is short-circuited. The size of this effect can be assumed equivalent to a parallel resistance R_{sh}. The equivalent circuit of a photovoltaic cell is shown in Fig. 1.

The output characteristic equation of the photovoltaic cell is defined as follows.

$$I = I_{ph} - I_D - I_{sh} \tag{1}$$

$$I_D = I_0 \left\{ \exp\left[\frac{q\left(U + I \cdot R_s\right)}{nKT} \right] \right\} \tag{2}$$

$$I_{sh} = \frac{U + I \cdot R_s}{R_{sh}} \tag{3}$$

By combining Eqs. (1)–(3), the *I–U* relation of the photovoltaic cell can be obtained as

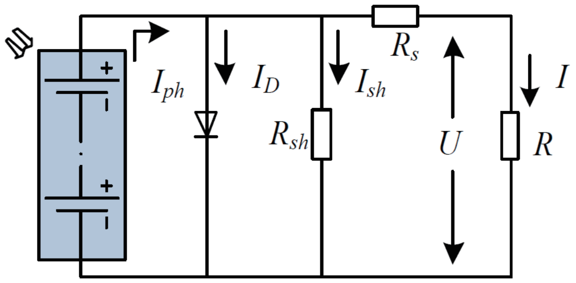

Fig. 1. (Color online) Equivalent circuit of photovoltaic cell.

$$I = I_{ph} - I_0 \left\{ \exp\left[\frac{q\left(U + I \cdot R_s\right)}{nKT} \right] \right\} - \frac{U + I \cdot R_s}{R_{sh}}, \tag{4}$$

where I_l is the photogenerated current (A), I_0 is the diode reverse saturation current (A), I and U are the output current (A) and output voltage (V) of the photovoltaic cell, n is the diode characteristic factor, K is the Boltzmann constant (1.38 × 10^{-23} J/K), q is the charge of an electron (C), T is the operating temperature of the photovoltaic cell (K), and R_s and R_{sh} are the series and parallel resistances of the photovoltaic cell, respectively (Ω).

2.3 Basic principle of MPPT

At a certain temperature and sunshine intensity, the relationship between the output current and the output voltage of the photovoltaic cell is nonlinear and has a unique MPP. In a photovoltaic power generation system, the output power of the photovoltaic cells must usually be kept at the maximum value, i.e., the photovoltaic cells work at the MPP, to improve their conversion efficiency and make full use of the luminous energy. However, factors such as the sunshine intensity and battery surface temperature vary from region to region, and sometimes change rapidly. Therefore, maintaining photovoltaic cells at the MPP in a constantly changing external environment has become an urgent and very important problem in photovoltaic power generation systems.[13] Because many unpredictable factors affect the output of the photovoltaic array, an adapter is required in photovoltaic power generation systems to coordinate the output power and circuit load. Therefore, a photovoltaic power generation system must be in a highly efficient and stable working state, providing the photoelectric conversion of the maximum power for the load, to improve the utilization of luminous energy. Figure 2 depicts the output characteristics of a photovoltaic cell at different temperatures and illumination intensities.

As can be seen from the *P–U* characteristic curves of the photovoltaic cell in Fig. 2, the MPP is not fixed at a point but is constantly varying within a range in response to the changes in the

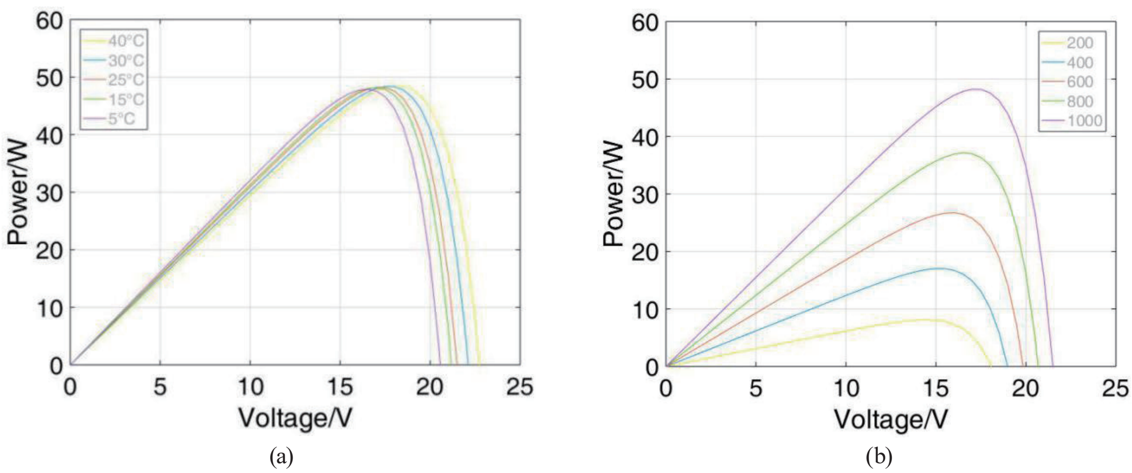

Fig. 2. (Color online) *P–U* characteristic curves of a photovoltaic cell at (a) different temperatures and (b) illumination intensities.

surrounding environment. The open-circuit current varies with the solar illumination intensity but the voltage corresponding to the MPP is unchanged. The MPPT algorithm is a technique that constantly adjusts the output impedance so that it equals the load impedance.

3. Proposed SVS-P&O Algorithm

3.1 Basic principle of P&O

P&O is suitable for the control system of a photovoltaic power generation system in a stable working environment. By making the system exhibit a certain dynamic response, the oscillation of the system output power near the MPP of photovoltaic cells can be reduced by reducing the disturbance step in the control algorithm. In addition, P&O, which is simple to operate, changes the voltage and current of the photovoltaic array continuously by perturbation, then calculates the output power by $P = UI$, and finally compares the two power values measured before and after the SVS-P&O. Figure 3 shows the P–U characteristic curve of a photovoltaic cell and its derivative. If the power value increases, a disturbance in the same direction is given. However, if the power value decreases, a disturbance in the opposite direction is given.

As shown in Fig. 3, P_k and P_{k-1} represent the current and previous sampling values, respectively. The disadvantages of P&O are as follows:

(1) The photovoltaic power generation system cannot consider both tracking accuracy and response speed. If the step size is too large, power fluctuation will occur, resulting in insufficient tracking accuracy; if the step size is too small, the tracking time will increase, and the system may operate at points with a low power output for a long time.

(2) The final result of the photovoltaic power generation system is continuous oscillation of its output in a small range near the MPP.

(3) When the external environment is constantly changing, the P&O will have large power fluctuations, and misjudgment may occur.

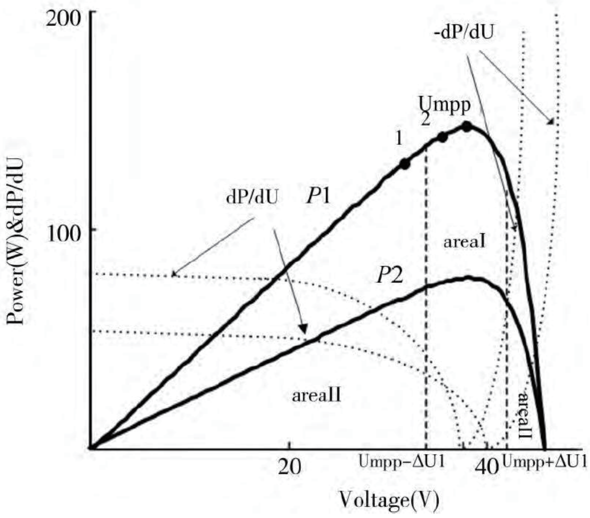

Fig. 3. P–U characteristic curve of the photovoltaic cell and its derivative.

3.2 SVS-P&O

P&O achieves MPPT by comparing power changes at the output end of the photovoltaic panel and adding perturbations to change the direction of power changes. When the output power of the photovoltaic cell detected at time $k + 1$ is greater than that detected at time k, the disturbance in the same direction will continue to be used, i.e., the output power will continue to be increased. Otherwise, a disturbance in the opposite direction will be adopted, i.e., the output power will be reduced. When the amount of disturbance is large and the external environment changes, although the MPP can be quickly tracked, oscillation near the MPP is generated. When the amount of disturbance is small and the external environment changes, the dynamic response of the system is slow. Therefore, the amount of disturbance selected is an important factor to measure in P&O.(14) When the output power of the photovoltaic cell is at the MPP, the derivative of the output power with respect to the working voltage is zero, i.e., $dP/dU = 0$.

In Fig. 3, curve P_1 represents an output power curve under stronger luminous intensity and curve P_2 defines an output power curve under weaker luminous intensity. The output P–U characteristic curve of the photovoltaic panel is divided into two areas, areas I and II. Area I is between the two vertical dashed lines and area II is outside the two vertical dashed lines. When the operating point of the system is in area I, which means that it is close to the MPP, a smaller perturbation step size (Step 1) is selected to reduce the fluctuation near the MPP. In contrast, when the system is in area II, the operating point is far from the MPP and a larger perturbation step size (Step 2) is adopted to track the MPP rapidly.

The power curve P_1 in Fig. 3 is taken as an example. The derivative of power P with respect to voltage U is shown in Table 1. The value of dP/dU on the left side of the MPP is smaller than the absolute value on the right side of the MPP. A value closer to dP/dU on the left and right sides of the MPP is smaller. Thus, the amount of disturbance can be adjusted by changing dP/dU, which is reflected in the MPPT circuit as the change in the duty cycle D.(15)

The detected voltages $U(k)$ and $U(k + 1)$ and currents $I(k)$ and $I(k + 1)$ at times k and $k + 1$, respectively, ΔU, and ΔP can be expressed as the following equations.

$$\Delta U = U\left(k+1\right) - U\left(k\right) \tag{5}$$

$$P\left(k\right) = U\left(k\right) \times I\left(k\right) \tag{6}$$

$$\Delta P = P\left(k+1\right) - P\left(k\right) \tag{7}$$

Table 1
Changes in value of *dP*/*dU*.

MPP	Left of MPP	Right of MPP
	0.67	−2.14
	0.65	−1.72
dP/*dU*	0.59	−1.20
	0.58	−0.84
	0	0

The perturbation amount in P&O can be expressed as

$$Step = N\left|\frac{dP}{dU}\right| = N\left|\frac{P(k+1)-P(k)}{U(k+1)-U(k)}\right|, \tag{8}$$

where *Step* is the perturbation step size and *N* is the velocity factor, which must satisfy $N < \frac{\Delta D_{\max}}{|dP/dU|}$.[16] In the MPPT algorithm, the duty cycle *D* is changed by changing the perturbation step size.[17]

$$D(k+1) = D(k) \pm Step \tag{9}$$

When the operating point of the system falls in area I, the step size of the SVS-P&O algorithm is changed. In contrast, when the operating point of the system falls in area II, the step size of the algorithm is fixed, i.e., $Step = \Delta D_{\max}$. The key to the algorithm is how to effectively convert two different disturbance steps, making it necessary to introduce a partition function to determine in which area of the system the operating point lies. The MPP of photovoltaic panels U_{mpp} has an approximately linear relationship with the open-circuit voltage U_{oc}:[18]

$$U_{mpp} = 0.81U_{oc}. \tag{10}$$

In addition, the partition function $F(x)$ is defined as

$$F(x) = \left|\frac{U(k)-U_{mpp}}{\Delta U_1}\right|. \tag{11}$$

It is found that $F(x) > 1$ and $F(x) \le 1$ represent the *P–U* characteristic curve of the photovoltaic cell in areas II and area I, respectively. The variation of the step size is analyzed in a specific external environment at a certain time, as shown in Figs. 3 and 4. At this time, the *P–U* output characteristic curve of the photovoltaic panel is curve P_1. When the photovoltaic power generation system is started, the SVS-P&O algorithm is initiated for control. The operating point of the system is at point 1 and judged to be in area I and far from the MPP by the partition function. Therefore, the algorithm moves towards the MPP with a large perturbation step size (Step 1) until the critical point between areas I and II is reached. Then, the partition function switches the perturbation step size to a small value (Step 2) and moves towards point 2, slowly approaching the MPP and reducing the oscillation near the MPP. The flow chart of the SVS-P&O algorithm is shown in Fig. 5. To reduce the design complexity of the algorithm, the photovoltaic power generation system is connected to a boost circuit, and impedance matching is realized by adjusting the duty cycle *D* of the pulse width modulation (PWM) signal in the boost circuit, thus realizing MPPT.

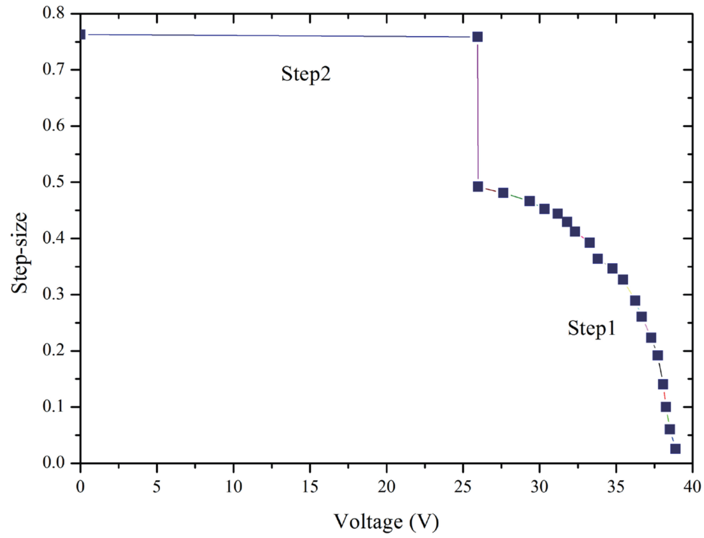

Fig. 4. (Color online) Variation of the step size.

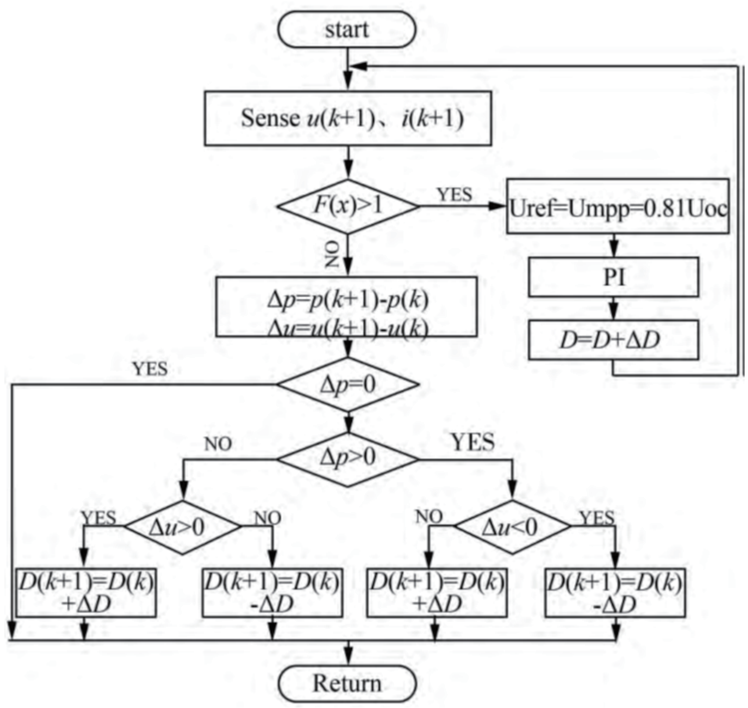

Fig. 5. Flow chart of SVS-P&O algorithm.

3.3 Implementation of boost circuit

The relationships between the input voltage U_i and output voltage U_o and between the input current I_L and output current I_o in the boost circuit in Fig. 6 are as follows:

$$U_i = U_o(1-D), \tag{12}$$

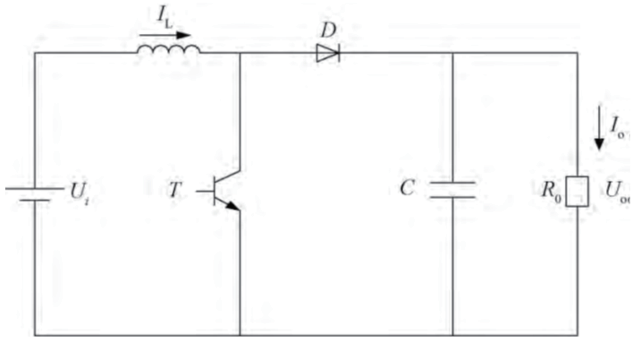

Fig. 6. Boost circuit.

$$I_o = I_L(1-D). \tag{13}$$

From Eqs. (12) and (13), we simultaneously obtain

$$R_i = \frac{U_i}{I_L} = \frac{U_o}{I_o}(1-D)^2 = R_o(1-D)^2, \tag{14}$$

where R_0 is a constant value. When D is changed, R_i is also changed. When R_i matches the output impedance of the photovoltaic array, MPPT can be realized.

4. Results and Discussion

4.1 Parameter setting

To verify the correctness of the SVS-P&O algorithm, a simulation model was built in MATLAB/Simulink, and an M function embedding was written to simulate the waveform of the photovoltaic power generation system under the application of the P&O and SVS-P&O algorithms. The circuit simulation parameters are shown in Table 2.

Table 2
Circuit simulation parameters.

Parameter	Value
Maximum power	175 W
Open-circuit voltage	38.2 V
Short-circuit current	6.2 A
Voltage at MPP	37.5 V
Current at MPP	4.95 A
Inductance	3 mh
Load resistance	50 Ω
Capacity	300 uF
Switching frequency	18 kHz

4.2 Analysis of results

At the temperature of 25 °C, the luminous intensity changes from 1000 to 600 W/m^2 at 0.5 s and from 600 to 800 W/m^2 at 1.0 s. Under the same external conditions, the two algorithms before and after the improvement are separately used for simulation. The simulation results are shown in Fig. 7. Figure 7(a) shows the waveform obtained with the traditional P&O simulation waveform,[9] and Fig. 7(b) depicts the simulation waveform obtained with the proposed SVS-P&O algorithm. When the photovoltaic power generation system is started, the time required by the traditional P&O algorithm to track the MPP is more than 0.03 s, while that required by the SVS-P&O algorithm is less than 0.02 s, and the output power stabilizes near the MPP after 0.02 s. The dynamic response speed of the SVS-P&O algorithm is higher than that of the traditional P&O algorithm. The average output power of the photovoltaic panels is 175.4 W at 1000 W/m^2, 150.5 W at 800 W/m^2, and 110.3 W at 600 W/m^2. The SVS-P&O algorithm improves the tracking accuracy of the MPPT while improving the efficiency of the photovoltaic power generation system.

To verify the operation of the SVS-P&O algorithm, an experimental prototype with a power of 500 W was built. Figure 8 shows the voltage and current waveforms output by the prototype when using the algorithm. The experimental waveforms show that the SVS-P&O algorithm can be applied to MPPT and is easy to implement, giving it high applicability in practical engineering.

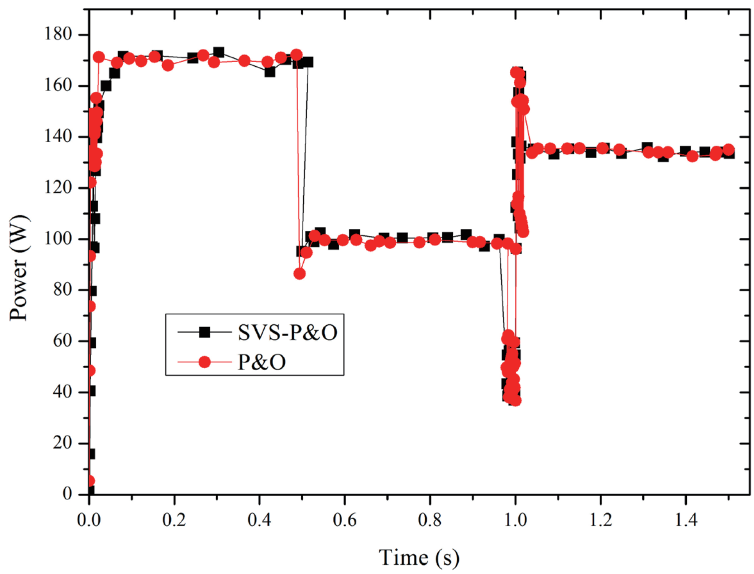

Fig. 7. (Color online) Simulation waveforms of different algorithms.

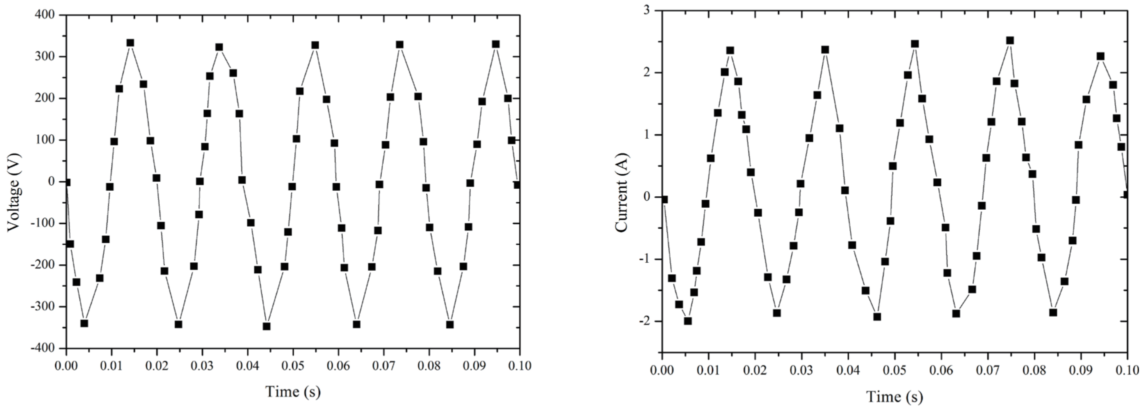

(a) (b)

Fig. 8. Test waveforms of output voltage (a) and current (b) for the prototype.

5. Conclusions

In this paper, we propose a novel SVS-P&O algorithm based on the existing research of P&O to solve the problem that the perturbation step size is too large or too small in P&O. This algorithm can solve the shortcomings of the traditional P&O step size adjustment process and avoid system judgment errors caused by the power fluctuation. The perturbation step size can be adjusted automatically, and the MPPT of the photovoltaic system can be realized by controlling the duty cycle of the boost circuit. When the external environment changes, the tracking accuracy and response speed of the system can be considered at the same time, and the SVS-P&O algorithm is advantageous over the conventional algorithm in the implementation of MPPT. The simulation results demonstrate the feasibility and reliability of the proposed algorithm.

Acknowledgments

This work was supported by the Science and Technology Research Project of Chongqing Education Commission (KJQN201803105) and Chongqing Science and Technology Commission (cstc2018jscx-msybX0270).

References

1 U. Yilmaz, O. Turksoy, and A. Teke: Int. J. Electr. Power Energy Syst. **113** (2019) 634. https://doi.org/10.1016/j.ijepes.2019.05.074
2 M. A. H. Ammar, B. Benhaoua, and M. Balghouthi: Energy Convers. Manage. **106** (2015) 31. https://doi.org/10.1016/j.enconman.2015.09.013
3 Y. H. Ji, D. Y. Jung, J. G. Kim, J. H. Kim, T. W. Lee, and C. Y. Won: IEEE Trans. Power Electron. **26** (2011) 1001. https://doi.org/10.1109/TPEL.2010.2089537
4 S. Bhattacharyya, D. S. K. Patnam, S. Samanta, and S. Mishra: IEEE Trans. Sustainable Energy **12** (2021) 293. https://doi.org/10.1109/TSTE.2020.2991768
5 P. Manoharan, U. Subramaniam, S. B. Thanikanti, P. Sanjeevikumar, and S. Ravichandran: IEEE Syst. J. **15** (2021) 3024. https://doi.org/10.10.1109/JSYST.2020.3003255
6 Q. Tian, G. Zhou, M. Leng, G. Xu, X. Fan, and T. Yan: Int. J. Circ. Theor. Appl. **49** (2021) 1. https://doi.org/10.1002/cta.3043

7 A. F. Mirza, M. Mansoor, K. Zhan, and Q. Ling: Energy **228** (2021) 120602. https://doi.org/10.1016/j.energy.2021.120602
8 T. Xu, F. Gao, P. Tan, X. Meng, and F. Blaabjerg: IEEE Trans. Power Electron. **35** (2020) 11281. https://doi.org/10.1109/TPEL.2020.2982763
9 F. Liu, K. Li, K. Chen, and Z. Zhao: IEEE J. Emerging Sel. Top. Power Electron. **8** (2020) 1287. https://doi.org/10 1109/JESTPE.2019.2942101
10 C. Wang, C. Zhu, G. Wei, J. Zhang, and F. Liu: IEEE Access **9** (2021) 45189. https://doi.org/10.1109/ACCESS.2021.3066805
11 M. Rezkallah, A. Chandra, M. Tremblay, and H. Ibrahim: IEEE Trans. Sustainable Energy **10** (2019) 181. https://doi.org/10.1109/TSTE.2018.2829213
12 D. Bernardi, E. Pawlikowski, and J. Newman: J. Electrochem. Soc. **132** (1985) 5. https://doi.org/10.1149/1.2113792
13 L. Tang, X. Wang, W. Xu, C. Mu, and B. Zhao: Sol. Energy **220** (2021) 523. https://doi.org/10.1016/j.solener.2021.03.047
14 Y. Li, X. Yuan, J. Li, H. Xiao, Z. Xu, and Z. Du: IET Gener. Transm. Distrib. **15** (2021) 1613. https://doi.org/10.1049/gtd2.12121
15 A. N. Ali, K. Premkumar, M. Vishnupriya, B. V. Manikandan, and T. Thamizhselvan: Sol. Energy **220** (2021) 473. https://doi.org/10.1016/j.solener.2021.03.077
16 D. Mitchell, N. Ye, and H. D. Sterck: Numer. Linear Algebra Appl. **27** (2020) e2297. https://doi.org/10.1002/nla.2297
17 X. Ye, Y. Tang, and D. Shu: IET Gener. Transm. Distrib. **14** (2020) 2890. https://doi.org/10.10.1049/iet-gtd.2019.1005
18 K. Osmani, A. Haddad, T. Lemenand, B. Castanier, and M. Ramadan: Energy **224** (2021) 120092. https://doi.org/10.1016/j.energy.2021.120092

About the Author

Xiaoping Lei received her B.S. degree from Chongqing Normal University, China, in 2007 and her M.S. degree from Chongqing University in 2012. She joined Chongqing College of Electronic Engineering, where she is currently a lecturer. Her research interests include circuit systems, automation, and IoT. (xiaopingleilei2@163.com)